Spike Latency Coding in a Biologically Inspired Micro-Electronic Nose

Hung Tat Chen, Kwan Ting Ng, *Student Member, IEEE,* Amine Bermak, *Senior Member, IEEE,* Man Kay Law, *Student Member, IEEE,* and Dominique Martinez

***Abstract*—Recent theoretical and experimental findings suggest that biological olfactory systems utilize relative latencies or time-to-first spikes for fast odor recognition. These time domain encoding methods have been demonstrated to exhibit reduced computational requirements and improved classification robustness [9], [12]. In this paper, we introduce a microcontroller (MCU) based electronic nose system using time domain encoding schemes to achieve a power efficient, compact and robust gas identification system. A compact (4.5cm×5cm×2.2cm) electronic nose, which is integrated with a tin oxide gas sensor array and capable of wireless communication with computers or mobile phones through Bluetooth, was implemented and characterized using three different gases (ethanol, carbon monoxide and hydrogen). During operation, the readout circuit digitizes the gas sensor resistances into a concentration independent spike timing pattern, which is unique for each individual gas. Both sensing and recognition operations have been successfully demonstrated in hardware. Two classification algorithms (rank-order and spike-distance) have been implemented. Both algorithms require no explicit knowledge of the gas concentration to achieve simplified training procedures, and exhibit comparable performances with conventional pattern recognition algorithms while enabling hardware friendly implementation.**

***Index Terms*—Neuromorphic engineering, olfactory system, Electronic nose, Gas Sensors, Spiking neurons.**

I. Introduction

THE biological olfactory system shows powerful and efficient odor discrimination capabilities. Mice and bees for example can recognize learned odors in less than 200 ms [1], [2], [3], [4], thereby indicating a rapid processing of the olfactory input. In the context of fast processing, neurons rely on processing only one spike per neuron, using relative latencies or time-to-first spikes after stimulus onset as an information carrier [5], [6]. In latency coding, one considers the neurons as analog-to-delay converters: the most strongly activated ones tend to fire first, whereas more weakly activated cells fire later or not at all. Under these conditions, the relative timing in which the cells fire their first spike is used as a code [7]. Evidence for latency coding has been found in the visual system[6], [10], the tactile system [11] and the olfactory system [4], [8]. Latency coding makes sense only if one considers the first spike with respect to a reference signal: the first spike after stimulus onset, or after a particular event in the stimulus dynamics. In the visual system, sudden movements of the eyes (i.e. saccades) sample the visual input into discrete snapshots. After each saccade, a new image is encoded into neural activities to be further processed by the brain. Similar to the saccades in vision, sniffing might provide an external reference in olfaction. Principal cells in the rat olfactory bulb exhibit a slow subthreshold oscillation that is phase-locked to the respiration [8]. The latency or time-to-first spike of these neurons with respect to the respiratory cycle decreases with odour concentration in a logarithmic way. Logarithmic encoding in the time domain has been previously proposed for solving the analog match problem in olfaction, i.e. recognize an odor irrespective of its concentration [9]. Theoretical works in [9] and [12] have highlighted the computational advantages of the biologically inspired time domain encoding scheme, namely the absence of computationally expensive normalization, the possibility of hierarchical classification and the tolerance to missing or inaccurate information.

In this paper, we introduce a microcontroller (MCU) based electronic nose system capable of real-time processing of sensor data, recognizing gases and wirelessly communicating with various platforms using Bluetooth. Logarithmic time domain encoding scheme is employed due to its reduced computation overhead. As a consequence, a low cost, power efficient, compact and robust gas identification system can be achieved. We have constructed a micro-electronic nose (E-nose) system with in-house fabricated metal-oxide sensors and logarithmic spike encoding adapted to the power law sensor response. A data acquisition technique based on resistance-to-time conversion is implemented to simplify the analog-to-digital conversion, hence enabling power consumption and system volume reduction. The whole system is implemented as a multi-chip platform. Data processing is accomplished through the MCU to enable real-time gas sensing and recognition functionalities. The system was characterized using three different gases (ethanol, carbon monoxide and hydrogen) for performance evaluation. It is also validated by comparing with conventional pattern recognition algorithms. Parameter extraction when training a new gas requires no explicit knowledge of the gas concentration, hence greatly simplifying the training procedure.

This paper is organized as follows. Section II demonstrates the logarithmic spike encoding scheme using our in-house metal oxide gas sensors. Section III describes the hardware implementation of the proposed E-nose system. Section IV

H. T. Chen, K. T. Ng, A. Bermak and M. K. Law are with the Department of Electronic and Computer Engineering, Hong Kong University of Science and Technology, Hong Kong, China (e-mail: sunchen@ece.ust.hk; kashng@ece.ust.hk; eebermak@ece.ust.hk; eeml@ece.ust.hk). K. T. Ng is also affiliated with the School of Electrical, Electronics and Computer Engineering, The University of Western Australia, Australia.

Dominique Martinez is with the CORTEX Group, LORIA-CNRS, Nancy, France (email: dominique.martinez@loria.fr). He is also affiliated with the UMR 1272, PISC-INRA, Versailles, France.

presents the resolution and noise analysis of the readout circuit. Section V illustrates the experimental measurements for both sensing and recognition. Finally, a conclusion is outlined in Section VI.

II. Spiking Metal Oxide Sensors

Metal oxide (MOx) sensors consist of a metal-oxide semiconducting film, mainly tin-dioxide (SnO_2), heated at an adequate temperature. The resistances of the devices change in the presence of a reducing or oxidizing gas. The sensitivity of a MOx sensor is defined as the ratio of the steady state resistance when the sensor is exposed to analytic gases over the baseline resistance when the sensor is exposed to dry air. It has been shown both experimentally and theoretically that the sensitivity of a MOx sensor to a given gas follows a power law at relatively high concentrations [13],[14],[17]. For an array of n MOx sensors, we then have

$$x_{i,j} = \frac{(R_s)_{i,j}}{(R_s)_{i,air}} \approx \alpha_{i,j}\, C_j^{r_{i,j}} \tag{1}$$

where i represents the ith sensing element of the sensor array ($i = 1, \cdots, n$) and j represents the tested gas with a given concentration C_j. The parameters $\alpha_{i,j}$ and $r_{i,j}$ depend on both the sensor parameters and the tested gases.

In order to discriminate between gases, the MOx sensor array has to be trained. Taking the logarithm of Eq. (1) has the benefit of linearizing the sensitivities. Yet the exponent parameter ($r_{i,j}$) for each sensor i has to be estimated for suitable calibration with a given gas j. This calibration procedure is usually fulfilled by fitting Eq. (1) to the sensor responses versus gas concentration. This estimation however requires an accurate control of the gas concentration, resulting in an expensive and complex calibration system. In order to solve this major issue, we propose to substitute the estimation of the exponent $r_{i,j}$ by using a new relative parameter defined as

$$a_{i,j} = \frac{r_{i,j}}{< r_j >} \tag{2}$$

with $< r_j >= \frac{1}{n}\sum_k r_{k,j}$ being the average over the n sensors. Taking the logarithm of Eq. (1) and extracting the log concentration leads to

$$\log C_j = \frac{1}{r_{i,j}}(\log x_{i,j} - \log \alpha_{i,j}) \tag{3}$$

Similarly, we have

$$\log C_j = \frac{1}{< r_j >}(< \log x_j > - < \log \alpha_j >) \tag{4}$$

with $< . >$ being the average over the sensors. From Eqs. (2), (3) and (4), the logarithmic sensitivity of the i^{th} sensor can be expressed as

$$\log x_{i,j} = a_{i,j} < \log x_j > + b_{i,j} \tag{5}$$

with $b_{i,j} = \log \alpha_{i,j} - a_{i,j} < \log \alpha_j >$. As a result, the parameter $a_{i,j}$ is extracted by calculating the slope of Eq. (5). The estimation of the parameters only requires to plot the log sensitivity of the i^{th} sensor versus the average log sensitivity. As no explicit knowledge of the concentration of the trained gas, the training procedure is thereby greatly simplified.

Hereafter we consider the MOx sensor array trained with the gas j. We propose to use the parameters $a_{i,j}$ to convert the outputs of the sensors into logarithmic spike timings, as observed in the biological system. Two methods have been proposed for gas identification in this paper, namely the rank order algorithm and the minimum spike distance algorithm.

For the rank order gas identification algorithm, each sensor produce a single spike at time $t_{i,g}$ expressed in arbitrary units (a.u) and given by

$$t_{i,g} = \frac{\log x_{i,g}}{a_{i,j}} \tag{6}$$

If the unknown gas g corresponds to the calibrated gas j, the relative spike timing is unique and independent of gas concentration. Using Eqs. (5) and (6) with $g = j$, the relative spike timing between the p^{th} and the q^{th} sensors can be written as

$$\begin{aligned} t_{p,j} - t_{q,j} &= \frac{\log x_{p,j}}{a_{p,j}} - \frac{\log x_{q,j}}{a_{q,j}} \\ &= \frac{b_{p,j}}{a_{p,j}} - \frac{b_{q,j}}{a_{q,j}} \end{aligned} \tag{7}$$

The first line of Eq. (7) shows that the calculation of the relative spike timing uses only $a_{i,j}$. Hence, the proposed algorithm is simple as only 1 parameter is required for each sensor. The resultant relative spike timing can also be represented by the last line of Eq. (7), which is independent of the concentration C_j. As a result, the unknown gas g is identified by comparing the firing sequence to the spike train prototype of the trained gas j.

For the minimum spike distance algorithm, it calculates the distance between the spike trains of the unknown gas g and trained gas j by

$$d(g,j) = \sum_i \left|\widetilde{t}_{i,g} - \widetilde{t}_{i,j}\right| \tag{8}$$

where $\widetilde{t}_{i,.} = t_{i,.} - \min(t_{p,.})$ is the relative spike timing of the i^{th} spiking sensor. The unknown gas g is classified as j whenever $d(g,j)$ is below a given discrimination threshold. These approaches greatly reduce the computational complexity associated with conventional machine learning methods for gas sensor array [15], thereby enabling the development of a compact electronic nose systems.

III. Electronic Nose System Implementation

A 4×4 tin oxide gas sensor array was designed and fabricated using an in-house 5 μm, 1-metal, 1-poly CMOS process [16], [17]. The cross section view of the fabricated sensor with micro-heater and electrodes is shown in Fig. 1(a). The

micro-machined micro-hotplate (MHP) is at the center of the sensor with a dimension of 190×190 μm^2. A 2.8 μm low-temperature-oxide (LTO) is formed by etching a sacrificial polysilicon layer [16]. This air gap prevents the heat leaks into the substrate, hence improving the heating efficiency. The SnO_2 sensing film is deposited onto the MHP using a sputtering method. Post-treatments were performed on 3 columns and 3 rows of the 4×4 sensor array as shown in fig. 1(b). Three different metal catalysts (Pt, Pd and Au) were deposited, one for each column while three different ion implantations (B, P and H) were performed, one for each row.

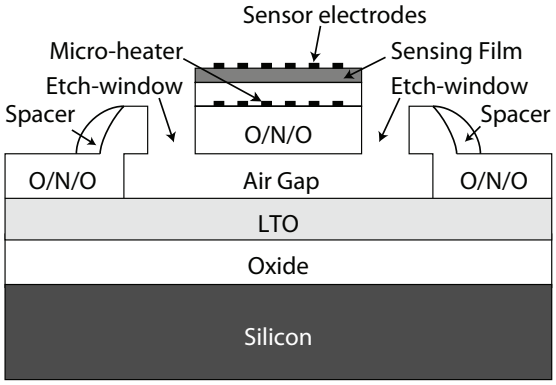

(a)

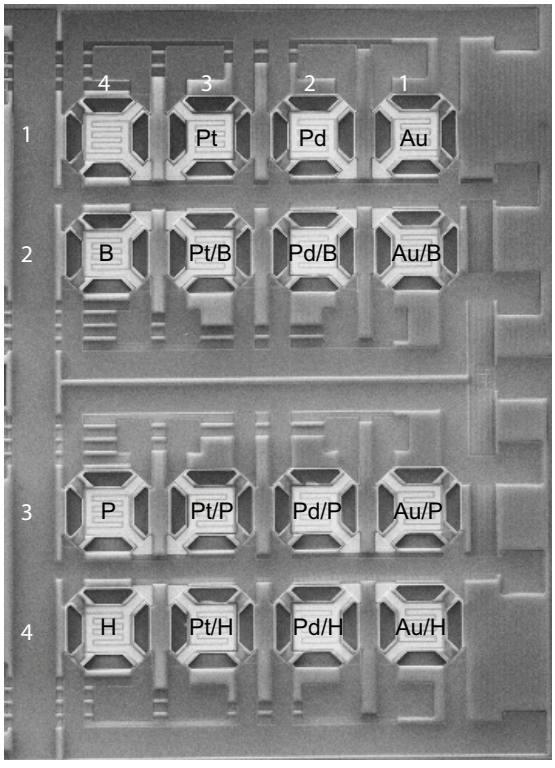

(b)

Fig. 1. (a) Cross section of the sensor element. (b) Microphotograph of the fabricated 4×4 gas sensor array using our in-house 5μm 1 metal, 1-poly CMOS process. The catalysts/ion implantations have been marked on the sensors accordingly.

In most reported electronic noses, the sensor resistances are evaluated by measuring the voltage across a potential divider and being digitized using an analog-to-digital converter (ADC) [20], [21]. However, this method suffers from low dynamic range because the sensor resistance typically ranges from $k\Omega$ to $M\Omega$ (depending on different fabrication processes). Moreover, the use of an ADC increases cost, system volume and power consumption. To address these limitations, we have implemented the readout approach as depicted in Fig. 2. This approach adds only one extra capacitor into the system to achieve digitization. All other required functional blocks are embedded in the MCU, which is already utilized for data processing and control. Hence the cost and the system volume can be reduced. The digitization process starts by charging the capacitor (C_m) up to a fixed voltage V_0. The analog multiplexer (MUX) subsequently selects a sensor and connects it to C_m in parallel. This capacitor C_m then discharges through the selected sensor resistance. When the capacitor voltage goes below the comparator threshold V_{th}, the MCU stops its internal timer, and the threshold crossing time (t_{cross}) can be expressed as

$$t_{cross} = R \cdot C_m \ln \frac{V_0}{V_{th}} \tag{9}$$

If we quantize t_{cross} with a clock frequency f_{clk}, the corresponding number of counts N can be expressed as

$$t_{cross} = \frac{N}{f_{clk}} \tag{10}$$

By using Eq. (9) and (10), and rearranging the terms, N can be expressed as

$$N = (C_m f_{clk} \ln(\frac{V_0}{V_{th}}))R_s = kR_s \tag{11}$$

where k is the discharging constant.

In contrast with the conventional approach that uses a current source for discharging an integrating capacitor, our circuit does not require an extra current source to perform conversion. As a result, the system volume and power consumption can be reduced, as there is no need for an extra building block to generate the reference current. Measurement results of the sensor array show that the embedded 16 bits timer available in the MCU is adequate for this system. The resolution and noise analysis of the readout circuit will be discussed in section IV in detail.

Fig. 3(a) illustrates the overall architecture of the E-nose system. It consists of the 4×4 SnO_2 gas sensor array, the resistance-to-time readout circuit with spike encoding using MCU and a Bluetooth module. A photo of the E-nose system is shown in fig. 3(b). The sensed gas is converted into spike timings according to Eq. (6) by the MCU. The generated spike train is then transmitted wirelessly to a personal computer, a Personal Digital Assistant (PDA) or a mobile phone for gas identification. The recognition algorithm was implemented both on a PC/PDA using Microsoft Visual Basic and on a mobile phone Nokia N95 using python for Symbian S60. It should be noted that the recognition algorithm can also be implemented on the MCU and only the final results will be transmitted to the mobile phone when needed. By implementing the algorithm in PC/mobile phone instead of

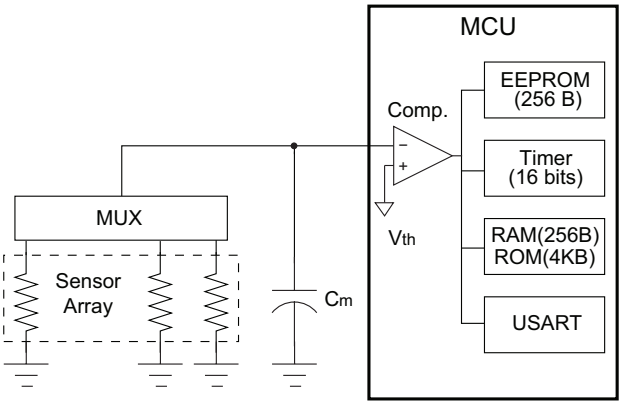

Fig. 2. Diagram of the resistance-to-time readout circuit. It utilizes the MCU comparator, with only one extra capacitor and one analog MUX added into the system. Note that the internal reference from the MCU is used to generate V_{th} to fully utilize the MCU available resources.

MCU, more functionalities can be included as the computational power of the MCU is limited. This is, however, not necessary in practical situations because in some applications, only the identification results are needed. Table I summarizes the overall E-nose system. It occupies a volume of 4.5cm×5cm×2.2cm and consumes a total current of 30mA at 5V supply for the overall system excluding the sensor array. In order to optimize the sensing performance of the fabricated gas sensor, operating temperature at 300^{o}C has been chosen. The proposed processing and implementation schemes are not limited to SnO_2 sensors. They can be applied to other gas sensor arrays with slight modification to the algorithm. The reason for utilizing SnO_2 as the sensing material is its high sensitivity to a wide range of gases, which is suitable for gas identification. The system was implemented using a *16F648A* MCU with embedded comparator and timer, a 16-channel analog multiplexer *HEF4067*, a Bluetooth module *T9JRN41-1* and a 0.01μF discrete capacitor. The estimated fabrication cost is about 25 USD.

TABLE I
SUMMARY AND MAJOR COMPONENTS OF THE E-NOSE SYSTEM.

Size	4.5cm×5cm×2.2cm
Power Consumption	322mW (Sensor array) 150mW (Other components)
Cost	USD25
Major Components	MCU (16F648A) × 1 MUX (HEF4067) × 1 Bluetooth (T9JRN41-1) × 1

IV. READOUT CIRCUIT RESOLUTION AND NOISE ANALYSIS

In the proposed system, the resolution requirement is mainly limited by the rank order gas identification algorithm. The correctness of the rank order classification depends on the successful differentiation of two nearby spikes, which in turn depends on the difference in sensor resistances. Measurements show that the minimum difference in sensor resistance ΔR is about 300Ω. Also, the maximum resistance R_{MAX}, which is

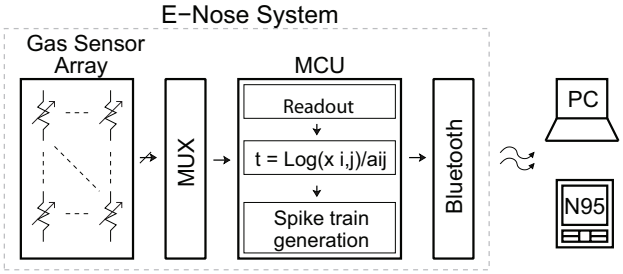

(a)

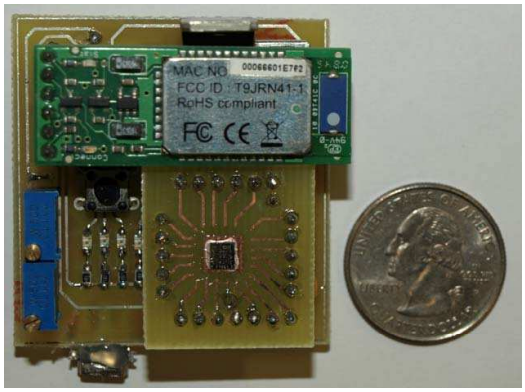

(b)

Fig. 3. (a) System overview of the E-nose system. Sensor resistances are digitized and processed in the MCU then transmitted to PC/Mobile phone (Nokia N95 in this work) for identification (b) The fabricated E-nose prototype with a US quarter dollar aside demonstrating its compactness.

about 400kΩ, is used to set the upper bound for digitization. As a result, the resolution required, which is defined as the ratio between R_{MAX} and ΔR, is approximately 11bits.

The clock frequency is determined by using the ΔR requirement for the RC readout circuit. The quantization clock period Δt is given by

$$\Delta t = \Delta R C_m \ln \frac{V_0}{V_{th}} \tag{12}$$

For C_m = 0.01μF, ΔR ≈300Ω, V_0 = 5V and V_{th} = 0.625V, Δt can be calculated to be approximately 6.24μs, and hence a clock frequency of 160kHz should be used. However, this clock speed also determines the speed of the MCU. Note that we try to fully utilize the MCU resources by utilizing the embedded 16 bit timer for quantization. In that case a 4MHz clock is used instead, as the 16 bit timer will still not be overflowed. One should note that even though 16 bit representation of the sensor resistance is available, only the 11 most-significant-bits (MSBs) are utilized for classification. It is worthwhile to mention that this requirement can be relaxed for a full-custom implementation leading to more room for overall power saving.

In order to achieve 11 bit resolution, the discharge curve and the reference voltage V_{th} should have at least 11 bit resolution. For the discharge curve, the measured achievable resolution is about 8 bit due to leakage current at the integration node. However, 11 bit resolution is required for the proposed system. To overcome this issue, multiple sampling and data averaging over every 8 samples are used to suppress the wide-band noise so as to restore the 11 bit resolution for identification.

For the reference voltage, the internal reference voltage provided by the MCU was used to fully utilize the available resources. This reference is in fact a resistor divider chain, and hence the reference voltage is dependent on the supply voltage. In that case, we regulated the supply voltage to ensure that it can achieve 11 bit resolution. As a result, the required resolution for the reference voltage V_{th} can be achieved. Notice that as the discharge curve is exponential, the resolution requirement should be determined when the capacitor voltage crosses V_{th}. This was achieved by differentiating the discharge curve with respect to time, (refer to fig. 2), which is

$$\begin{aligned}\frac{\delta V}{\delta t}|_{V=V_{th}} &= \frac{\delta}{\delta t}(V_0 e^{-\frac{t}{RC_m}})|_{V=V_{th}} \\ &= -\frac{V_0}{RC_m} e^{-\frac{t}{RC_m}}|_{V=V_{th}} \end{aligned} \quad (13)$$

where R is the equivalent resistance at the integration node and C_m is the integrating capacitance. By using Eq. (9) and (13), we obtain

$$\frac{\delta V}{\delta t}|_{V=V_{th}} = \frac{\delta V}{\delta t}|_{t=t_{cross}} = -\frac{V_{th}}{RC_m} \quad (14)$$

Hence, the corresponding voltage representation for 1 LSB is

$$|\Delta V| \approx \frac{V_{th}}{R \cdot C_m}\Delta t \quad (15)$$

The worst case occurs at $R = R_{MAX} \approx 400\text{k}\Omega$. For C_m = 0.01μF, V_{th} = 0.625V and Δt = 6.24μs (equivalent to 160kHz clock as the 5 LSBs of the 16 bit representation are not required). The tolerable noise level in voltage domain can be calculated to be roughly 975μV. Note that the thermal noise produced by the divider chain is negligible as a 1MΩ resistor should roughly generate a noise voltage much less than $1\mu V/\sqrt{Hz}$ at 300^{o}K. In that case, the requirement for the PSRR of the 5V supply can be determined to be roughly 74.2dB. Hence, the component LM317, which has 80dB PSRR, is selected to regulate the supply voltage in the proposed system.

V. Experimental Results

Characterization of the E-nose system has been performed at different stages. The sensor array was first characterized in a controlled condition to eliminate the unwanted effects from ambient environment. The readout circuit was subsequently tested with emulated resistors modeling the gas sensors. Finally, experiments were performed for the overall E-nose system, including the sensor array, the readout circuit, the MCU module and the Bluetooth module through a portable demo prototype.

A. Characterization of the gas sensor array

The gas sensor array was characterized in a laboratory environment with a gas delivery system as shown in fig. 4. It consists of 4 mass-flow-control (MFC) which controls the flow-rate of each gas. The gas concentration is adjusted by mixing the gas with air at different flow rates inside the chamber which contains the SnO_2 gas sensor array. The sensor responses are transmitted to a PC through a data acquisition board (DAQ), which is also responsible to control the gas flow as well as the heater temperatures of the sensors. Table II summarizes the sensor characteristics and the characterization setup. Three gases (hydrogen, ethanol and carbon monoxide) have been tested in the range between 20ppm and 200ppm during characterization.

TABLE II
Sensor array characteristics and characterization setup

Sensor array features				
Process	In-house 5μm			
Sensor array	4×4 SnO_2			
Catalysts	Pt, Pd and Au			
Ion implantation	B, P and H			
Operating temperature	∼300^{o}C			
Heater resistance	∼400Ω			
Power consumption (per sensor)	23mW			
Sensor characterization setup				
Chamber dimension	Radius = 2.5cm, Volume = 30cm^3			
Max gas flow rate	500ml/min			
Exposure time	250s			
Gas concentration range	20ppm to 200ppm			
Sensor resistances				
	Air	H_2	Ethanol	CO
Max	398 kΩ	152 kΩ	183 kΩ	355 kΩ
Min	13 kΩ	665 Ω	645 Ω	2.9 kΩ

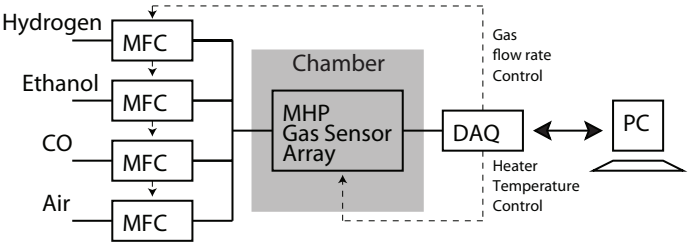

Fig. 4. Experimental setup used to characterize the sensor array.

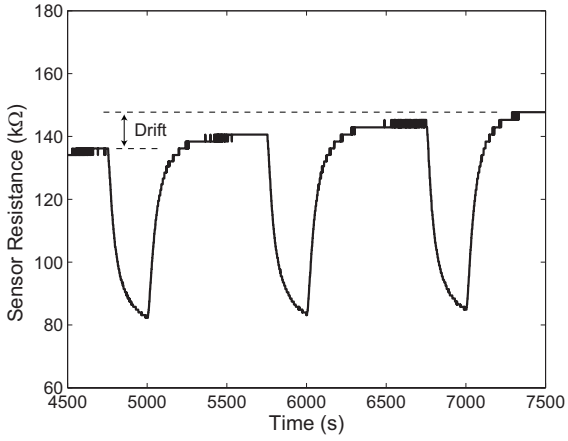

Fig. 5. Typical sensor response to ethanol. The sensor was initially exposed to air then exposed to ethanol for 3 times. It is exposed to air for sensor resistance recovery. Note that the sensor resistance is not able to fully recover to the original value due to drift.

Fig. 5 shows a typical sensor response during gas exposure. Notice that the sensor baseline resistance does not recover to its original value after exposure. This is known

as sensor baseline drift, which significantly complicates the identification process because of the low repeatability of the sensor responses. Drift is a common issue for gas sensors. It is due to aging, poisoning and other ambient environment fluctuations. Since sensor drifting is inevitable, the proposed gas identification methods are designed to be robust even when drift is present in the sensors.

B. Characterization of the Readout Circuit.

In practice, the performance of the resistance-to-time readout interface may be affected by a number of external parameters such as temperature, humidity, noise and gas flow. To characterize possible interference in real-world conditions, we used the readout circuit to measure two identical standard resistors (10kΩ) inside the chamber when a gas is injected. Fig. 6 shows the measurement results of the typical relationship between the normalized discharge constant *k* and two multiplexed channels when the two standard resistors are exposed to ethanol. One can observe that the normalized discharge constant (*k*) of both channels increases dramatically when ethanol is injected into the chamber at t=650s. In other words, the normalized discharge constant (*k*) depends on the injected gas. We, however, noticed that the values of *k* are correlated in the two channels. To compensate for this error, 2 standard resistors R_1 and R_2 are placed in 2 MUX channels. For each measurement, we sample these 2 resistances to extract the discharge constant *k* and to eliminate the internal resistance R_{MUX} of the multiplexer. Assume that *k* and R_{MUX} are similar for both channels, the counts obtained through this characterization can be expressed as

$$\begin{aligned} N_1 &= k(R_1 + R_{MUX}) \\ N_2 &= k(R_2 + R_{MUX}) \\ N_s &= k(R_s + R_{MUX}) \end{aligned} \tag{16}$$

where N_1, N_2 and N_s are the quantized values of the standard resistors R_1, R_2, and the sensor resistance R_s respectively. With this scheme, R_s can be extracted using

$$\begin{aligned} \frac{N_s - N_1}{N_2 - N_1} &= \frac{R_s - R_1}{R_2 - R_1} \\ R_s &= \frac{N_s - N_1}{N_2 - N_1}(R_2 - R_1) + R_1 \end{aligned} \tag{17}$$

Hence, the discharge constant and internal resistance of the multiplexer are compensated.

To characterize the error made during the sensor readout, the chemical sensors were emulated using resistors ranging from 1kΩ to 500kΩ (1/4W,1%), which are approximately equivalent to exposing our sensors to gases such as ethanol, CO or hydrogen between 20ppm and 200ppm concentration levels, to eliminate the effects of ambient environments. This resistance range is selected as it corresponds to the real gas measurements as stated in table II. The resistances were measured using a multi-meter with a resolution of 1mΩ. Fifty measurements for each sample were taken at room temperature. Fig. 7 shows the discharging count obtained from the timer in the MCU with different resistance values. It shows a very good linearity with a relative error of less than 0.4%.

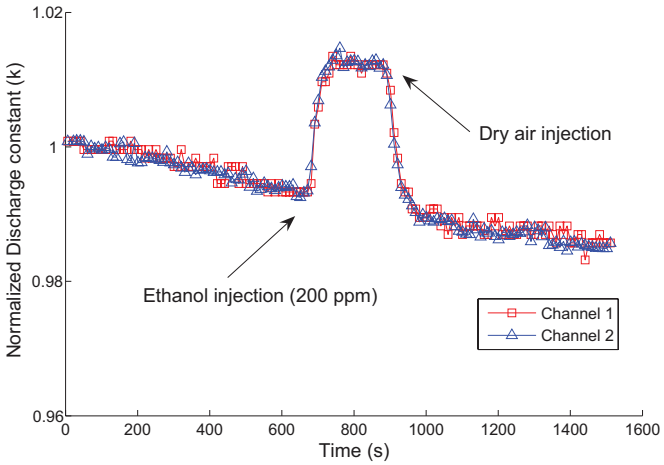

Fig. 6. Typical relationship between the normalized discharge constant *k* and two multiplexed channels when the two standard resistors are exposed to ethanol.

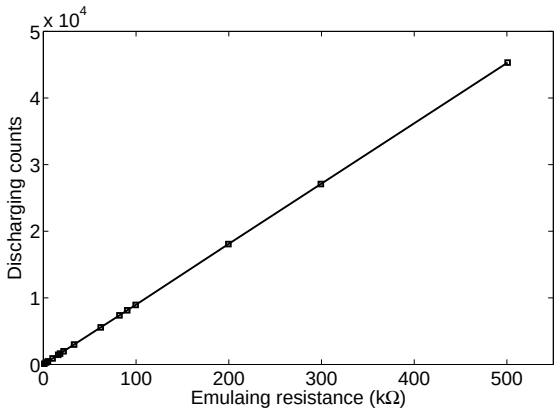

Fig. 7. Measured discharging count using different resistances for the readout circuit characterization.

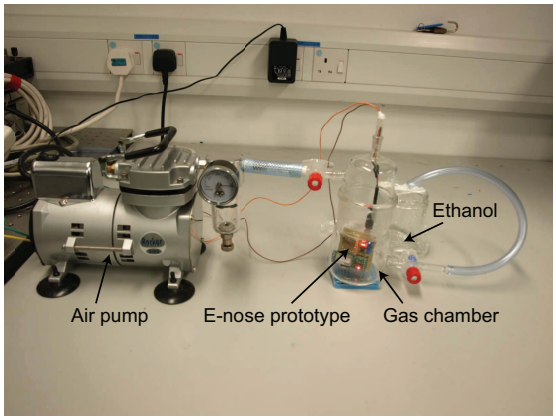

Fig. 8. Portable demo prototype. The compact E-nose system is placed inside a gas chamber. An air pump is connected to the gas chamber in order to provide a stable sensing environment for the system. Gas sensor resistances are first digitized then are transmitted to PC/PDA wirelessly using the Bluetooth module.

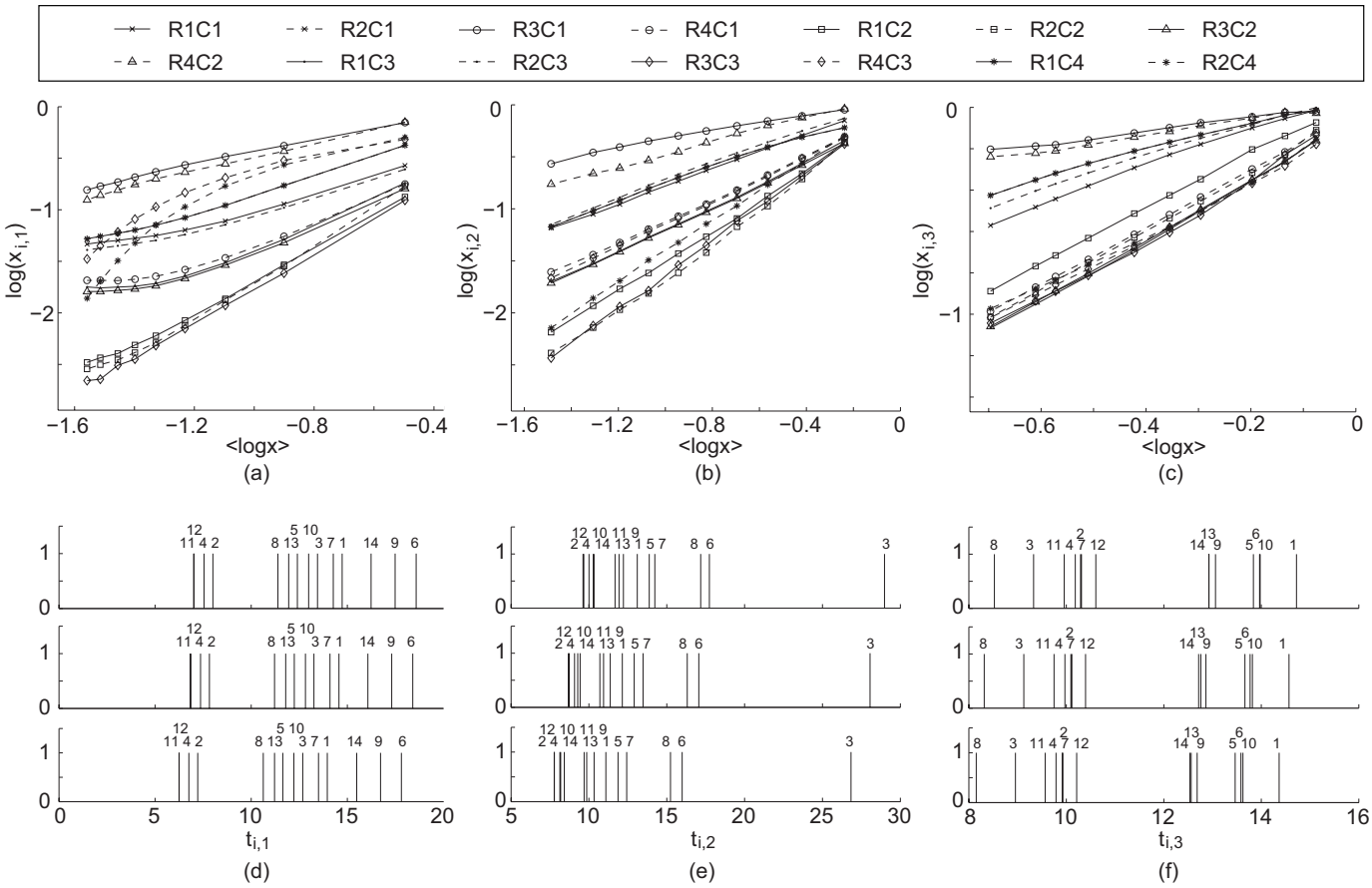

Fig. 9. Characterization results of the E-nose system to different gases: H_2, ethanol and CO from left to right. (a)-(c) Sensor sensitivities of 14 sensors, where RxCy represents the location of the sensor at row x column y. The slopes are used to calculate $a_{i,j}$ as stated in Eq. (5); (d)-(f) Typical spike trains obtained from exposure to gases at different concentration. Only a shift to the entire pattern is presented for concentration variation, which can be compensated in the proposed gas identification algorithms hence achieving concentration independent recognition.

C. Training and Testing of the Electronic Nose System

In order to test our E-nose system, we have built a portable demo prototype as shown in fig. 8. The E-nose system is placed inside a gas chamber which is connected to an air pump. During operation, gases are injected into the chamber. The system samples the gas by digitizing the sensor resistances. The quantized values are subsequently transmitted wirelessly to PC/PDA using the Bluetooth interface.

The E-nose system was trained on 3 different gases namely hydrogen, ethanol and carbon monoxide. Fig. 9(a) – (c) show the plots of the log sensitivity of the 14 sensors versus the average log sensitivity for different gases at concentrations ranging from 20ppm to 200ppm. Only 14 sensors were characterized because 2 channels are preserved for auto-compensation of the readout error, as explained in the previous section. The parameters $a_{i,j}$ are extracted by linear regression. Therefore, 14 parameters are obtained for each gas. These parameters are then used for spike encoding as discussed in Eq. 6. Fig. 9(d) – (f) report the spike trains generated for the 3 different analytic gases at different concentrations. As shown in the figures, a unique sequence can be observed for each individual gas regardless of its concentration. The unique spike trains for the trained gases are used later for gas identification. One should note that the absolute spike timings of the sequence decrease when gas concentration increases. However, the relative spike timings are preserved. Note that even though the proposed algorithms are concentration independent, the targeted gas concentration can still be extracted. As shown in Fig. 10, the absolute time of the first spike of the sequence is well correlated with the gas concentration. Therefore, the concentration information can be retrieved using absolute spike timings after the unknown gas is recognized. The proposed schemes convey two complementary informations, namely gas identity and concentration, which are encoded by the relative and the absolute spike timings, respectively.

To identify unknown gases, the spike trains generated by the E-nose system have to be compared to the stored prototypes of the trained gases. We trained our sensors in a ten-sample dataset with hydrogen, ethanol and carbon monoxide at concentrations ranging from 20ppm to 200 ppm. The encoding parameters a_{ij} were derived by computing the slope as shown in Eq. (5). A single spike train prototype per trained gas was extracted by averaging the relative spike timings over the training samples. To characterize the system robustness, we perform gas identification on another dataset of 440 samples. We tested two methods for gas identification. The first method relies on comparing the rank order of the generated spikes as in [17][22]. The second method relies on computing the

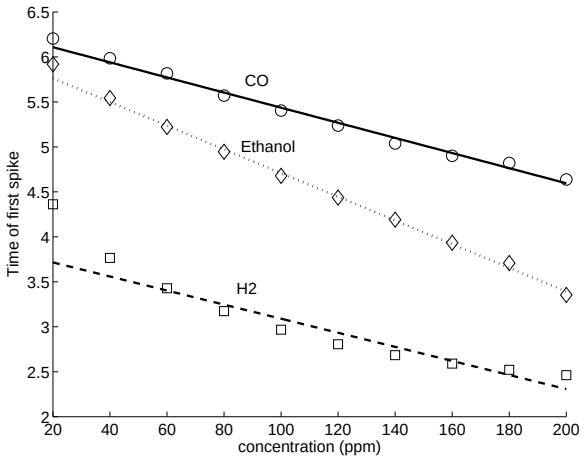

Fig. 10. Absolute time of the first spike of the generated spike train versus gas concentration, for ethanol, carbon monoxyde and hydrogen.

spike distance as given by Eq. (8). Relative spike distances were computed between the test patterns and the three stored prototypes and the test patterns were classified according to the minimum distance.

Table III compares the performance of the proposed recognition methods with other pattern recognition techniques including K-nearest neighbor (KNN), Multi-layer perception (MLP), Radial Basis Function (RBF), Gaussian Mixture Models (GMM) and Probabilistic Principal Component Analysis (PPCA). The identification performance of the rank order is the lowest among all recognition algorithms. This is because the generated spike trains could contain very close spikes so that a small spike jitter may induce large differences in the rank order. On the other hand, the spike distance measure leads to a perfect recognition and, despite its simplicity, outperforms KNN and RBF.

TABLE III
RECOGNITION PERFORMANCE FOR OUR SPIKING TECHNIQUE AS COMPARED TO SOME CLASSICAL PATTERN RECOGNITION ALGORITHMS.

Recognition Method	Classification Performance (%)
KNN	99.77
MLP	100
RBF	98.64
GMM	100
PPCA	100
Spike Rank order	95.2
Spike distance	100

VI. CONCLUSION AND FUTURE WORK

In this paper, we have presented a compact low cost electronic nose system integrating a 4×4 tin-oxide gas sensor array together with a biologically inspired spike encoding scheme. Both sensing and recognition operations have been successfully demonstrated in a MCU based hardware. A readout scheme based on resistance-to-time conversion is implemented, enabling the removal of an analog-to-digital converter, leading to reduced power consumption and system volume.

The proposed resistance-to-time readout interface is also optimized for real application scenarios where external parameters such as temperature, humidity, noise and gas flow can drastically affect the performance of the overall system. Calibration resistances are used to extract the discharge constant and eliminate the effect of gas flow and the effect of internal resistance R_{MUX} of the multiplexer, leading to a very good linearity with a relative error of less than 0.4%. The quantized resistances are processed into spike timings in the MCU. Classification is performed by examining the relative spike timings of the spiking sensors and any unknown gas is classified using spike pattern matching. This approach greatly reduces the computational complexity associated with conventional machine learning methods for classification. Parameter estimation when training a new gas does not require any explicit knowledge of the concentration of the trained gas. As a result, learning a new gas can be easily performed. Moreover, the parameter extraction is very simple and requires only limited computational power resulting in low cost and low power hardware implementation. Recognition performance of our proposed system is compared to classical pattern recognition algorithms and results illustrate the effectiveness of our proposed scheme. This work pioneers the translation of neurophysiological findings into hardware implementation for the processing of gas sensor data featuring a number of advantages such as simple recognition, easy calibration and training.

As most of the power is consumed by the sensor heater, energy saving schemes such as temperature modulation and sensor transient response readout could be applied on the sensor in the future to reduce the power consumed by the heater [18], [19]. To further reduce the power consumed by the sensor heater, sensors with room temperature sensing such as polymer or carbon nanotube sensors can be used. However, these sensors are more sensitive to ambient environment fluctuations as the sensing temperature is not controlled [23].

ACKNOWLEDGEMENTS

This research was funded by a grant from the Research Project Competition (RPC) at HKUST as well as the INRIA associated team BIOSENS (BIO-inspired SENSing) and by the project ”olfactory coding” from the Neuroinformatics program of the CNRS.

REFERENCES

[1] N.M. Abraham, H. Spors, A. Carleton, T.W. Margrie, T. Kuner and A.T. Schaefer, “Maintaining Accuracy at the Expense of Speed”, neuron, Vol 4(5), 2004, pp. 865-876.

[2] D.W. Wesson, T.N. Donahou, M.O. Johnson and M. Wachowiak, “Sniffing Behavior of Mice during Performance in Odor-Guided Tasks”, Chemical Senses, Vol 33(7), 2008, pp. 581-596.

[3] G.A. Wright, M. Carlton and B.H. Smith, “A Honeybee’s Ability to Learn, Recognize, and Discriminate Odors Depends Upon Odor Sampling Time and Concentration”, Behavioral Neuroscience. Vol 123(1), Feb 2009, pp. 36-43.

[4] S. Krofczik, R. Menzel and M.P. Nawrot, “Rapid odor processing in the honeybee antennal lobe network ”, Front. Comput. Neurosci. Vol 2(9). 2009.

[5] S. Thorpe, D. Fize and C. Marlot “Speed of processing in the human visual system”, Nature, Vol 381, 1996, pp. 520-522.

[6] T. Gollisch and M. Meister “Rapid neural coding in the retina with relative spike latencies”, Science, Vol 319, 2008, pp. 1108-1111.

[7] V. Rullen and S. J. Thorpe, “Rate Coding Versus Temporal Order Coding: What the Retinal Ganglion Cells Tell the Visual Cotex”, Neural Computation, 13, 2001, pp. 1255-1283.

[8] T. Margrie and A. Schaefer, “Theta Oscillation Coupled Spike Latencies Yield Computational Vigour in a Mammalian Sensory System”, Journal of Physiology, 546, 2003, pp. 363-374.

[9] J. Hopfield, “Pattern Recognition Computation Using Action Potential Timing for Stimulus Representation”, Nature, 376, 1995, pp. 33-36.

[10] T.J. Gawne, T.W. Kjaer and B.J. Richmond, “Latency: another potential code for feature binding in striate cortex”, Journal of Neurophysiology, Vol 76(2), 1996, pp. 1356-1360.

[11] R.S. Johansson and I. Birznieks “First spikes in ensembles of human tactile afferents code complex spatial fingertip events”. Nature Neuroscience, Vol 7(2), 2004, pp. 170-177.

[12] J. Hopfield, “Computing with action potentials”, Neural Information Processing Systems 10, 1998, pp. 166-172.

[13] Noboru Yamazoe and Kengo Shimanoe, “Theory of power laws for semiconductor gas sensors”, Sensors and Actuators B, 128, 2008, pp. 566-573.

[14] P. K. Clifford and D. T. Tuma, “Characteristic of Semiconductor Gas Sensors Part I: Study. State Gas Response”, Sensors and Actuators, Vol. 3, 1982-1983, pp. 233-254.

[15] A. Bermak, S. Belhouari, M. Shi, and D. Martinez, “Pattern Recognition Techniques for Odor Discrimination in Gas Sensor Array”, The Encyclopedia of Sensors, C.A. Grimes, E.C. Dickey and M.V. Pishko (eds.), American Scientific Publishers, Vol. 7, 2006, pp. 349-365.

[16] Bin Guo, Amine Bermak, Philip C.H. Chan and Guizhen Yan, “An Integrated Surface Micro-machined Convex Micro-hotplate Structure for Tin Oxide Gas Sensor Array”, IEEE Sensors Journal, Vol. 7, No. 12, Dec. 2007, pp. 1720 - 1726.

[17] Kwan Ting Ng; Bin Guo; Bermak, A.; Martinez, D.; Boussaid, F., “Characterization of a logarithmic spike timing encoding scheme for a 4×4 tin oxide gas sensor array”, IEEE Sensors conference, 2009, pp. 731 - 734.

[18] T. Amamoto, T. Yamaguchi, Y. Matsuura, Y. Kajiyama, “Develop- ment of pulse-drive semiconductor gas sensor”, Sensors and Actuators, B 13 - 14, 1993, pp. 587 - 588.

[19] Y. Kato, K. Yoshikawa, M. Kitora, “Temperature-dependent dynamic response enables the qualification and quantification of gases by a single sensor”, Sensors and Actuators, B, 40, 1997, pp. 33-37.

[20] Hyung-Ki Hong, Chul Han Kwon, Seung-Ryeol Kim, Dong Hyun Yun, Kyuchung Lee and Yung Kwon Sung, “Portable electronic nose system with gas sensor array and artificial neural network”, Sensors and Actuators B: Chemical, 66, 2000, pp 49-52.

[21] Yong Shin Kim, Seung-Chul Ha, Yoonseok Yang, Young Jun Kim, Seong Mok Cho, Haesik Yang and Youn Tae Kim, “Portable electronic nose system based on the carbon black-polymer composite sensor array”, Sensors and Actuators B: Chemical, 108, 2005, pp. 285-291.

[22] T. Chen, A. Bermak and D. Martinez “Towars a bio-inspired micro-electronic nose”, The 13th International Symposium on Olfaction and Electronic Nose ISOEN 2009, Brescia, Italy, 2009.

[23] D.Huang and H.Leung, “Reconstruction of drifting sensor response based on Papoulis-Gerchberg method, IEEE Sensor Journal, vol.9, no.5, 2009, pp.595-604.

Hung Tat Chen received his B.Sc. degree in the Department of Computer Engineering from Hong Kong University of Science and Technology (HKUST), Kowloon, Hong Kong, in 2007, and his Mphil. degree in the Department of Electronic and Computer Engineering at the same university in 2009.

He is currently with Appotech (HK) Limited working as a research engineer. His research interests include Electronic-nose micro-system and Bio-inspired spiking neural recognition algorithms.

Kwan Ting Ng (S’08) received his BE(Hons.) in Electrical and Electronics Engineering from The University of Western Australia in 2007. He is currently pursuing a double-badged Ph.D. degree in The University of Western Australia and Hong Kong University of Science and Technology. His research interests include mixed-mode integrated circuit design, smart CMOS vision sensors and integrated gas sensors. In June 2010, he was awarded the ”Best Student Paper Award” in the IEEE International Symposium on Circuits and Systems (ISCAS 2010).

Amine BERMAK (M’99-SM’04) received both his MEng and PhD degrees in Electronic Engineering from Paul Sabatier University, Toulouse, France in 1994 and 1998, respectively. During his PhD, Dr. Bermak was part of the Microsystems and Microstructures Research Group at the French National Research Center LAAS-CNRS where he developed a 3D VLSI chip for artificial neural network classification and detection applications. He then joined the Advanced Computer Architecture research group at York University, York, England, where he was working as a Post-doc on VLSI implementation of CMM neural network for vision applications in a project funded by British Aerospace.

In 1998, Dr. Bermak joined Edith Cowan University, Perth, Australia, first as a research fellow working on smart vision sensors, then as a lecturer and a senior lecturer in the school of Engineering and Mathematics. He is currently an Associate Professor with the Electronic and Computer Engineering Department of Hong Kong University of Science and Technology (HKUST) where he is also serving as the director of Computer Engineering and the director of MSc degree in Integrated Circuit Design (ICDE).

Dr. Bermak has received many distinguished awards, including the 2004 ”IEEE Chester Sall Award”; HKUST ”Engineering School Teaching Excellence Award” in 2004 and 2009; and the ”Best Paper Award” at the 2005 International Workshop on System-On-Chip for Real-Time Applications. Dr. Bermak is a member of technical program committees of a number of international conferences including the IEEE Custom Integrated Circuit Conference CICC’2006, CICC’2007, the IEEE Consumer Electronics Conference CEC’2007, Design Automation and Test in Europe DATE2007, DATE2008. He is the general co-chair of the IEEE International Symposium on electronic design test and applications, Hong Kong 2008, and the general co-chair of the IEEE Conference on Biomedical Circuits and Systems, Beijing, 2009. He is also on the editorial board of IEEE Transactions on VLSI systems; IEEE Transactions on Biomedical Circuits and Systems and the Journal of Sensors. Dr Bermak is a senior member of IEEE and a member of IEEE CAS committee on sensory systems. His research interests are related to VLSI circuits and systems for signal, image processing, sensors and microsystems applications. He has published extensively on the above topics in various journals, book chapters and refereed international conferences.

Man Kay Law (S’07) received his B.Sc. degree in the Department of Computer Engineering from Hong Kong University of Science and Technology (HKUST), Kowloon, Hong Kong, in 2006. He is currently pursuing his Ph.D. degree in the Department of Electronic and Computer Engineering at the same university.

His research interests include smart temperature sensors, CMOS image sensors, sensor readout circuit designs, integrated wireless sensing and biomedical systems, ultra-low power analog design techniques, and integrated energy harvesting techniques.

Dominique Martinez received his PhD degree in electrical and electronic engineering from the University Paul Sabatier in Toulouse, France, in 1992. He was a post-doctoral fellow at MIT, Dept. Brain and Cog. Sciences, and Harvard, VLSI group, in Cambridge, MA, USA, in 1992 and 1994, respectively. Since 1993, he has a permanent research position at the CNRS in France. From 1993 to 1999 he worked at LAAS-CNRS in Toulouse, France, where his research interests were concerned with machine learning. In 2000 he joined LORIA-CNRS in Nancy, France, and his research interests currently focus on computational neuroscience and olfaction (both biological and artificial). Since 2009, he is also affiliated with PISC-INRA, a biological laboratory in Versailles, France.